ISSN: 2414-1895 DOI: 10.6919/ICJE.202505_11(5).0005

Design of High-speed Permanent Magnet Motor for Energy Storage Flywheel

Xu Wang, Yongqi Li

School of Mechanical Engineering, Tianjin University of Technology and Education, Tianjin 300222, China

Abstract

As the core component of flywheel energy storage system, permanent magnet motors need to possess characteristics such as high efficiency, high torque and low heat generation to meet the performance requirements of the motor for the flywheel energy storage system. To achieve the above requirements, this paper designs an energy storage flywheel motor with a rated power of 500W and a rated speed of 10000r/min, and proposes a new stator-less coreless permanent magnet synchronous motor structure for energy storage flywheels. The rotor magnetic circuit of the motor is optimized through multi-objective design. Firstly, a simulation model of the new motor is established. Then, finite element analysis is conducted using Maxwell. Secondly, the rotor magnetic circuit is optimized using the improved NSGA-II algorithm. Finally, finite element simulation is built for verification. The research shows that the finite element simulation results indicate that, under the condition that the maximum envelope volume of the motor remains unchanged, the average output torque of the motor increases from 428.9 mN/m to 451.2mN/m, an increase of approximately 5.2%. The torque fluctuation decreases from 64.0 mN/m to 61.8 mN/m, a reduction of 3.4%. The new structure effectively reduces the heat generation of the motor and significantly improves the overall performance of the motor. It has certain reference significance for the design of permanent magnet motors for energy storage flywheels.

Keywords

Ironless Permanent Magnet Motor; Torque; Multi-objective Optimization.

1. Introduction

With the increasing global demand for energy and the vigorous promotion of energy conservation and emission reduction, the proportion of green energy such as wave energy, solar energy and wind energy has been increasing year by year. Due to the cyclical and intermittent characteristics of these green energies, the energy supply is unstable, which greatly restricts the development of green energy. To achieve stable green energy supply, energy storage technology has developed rapidly. Currently, the existing energy storage methods include battery energy storage (UPS), supercapacitor energy storage, flywheel energy storage, compressed air energy storage and pumped storage, etc[1-3].

Flywheel energy storage is currently a popular development direction in energy storage research. It realizes energy storage through the rotation of an internal flywheel, and belongs to a physical energy storage method. The performance of flywheel energy storage is not limited by external conditions and can achieve an energy conversion efficiency of about 85-95%. The storage time is about 20 minutes, and the lifespan is extremely high, making it highly suitable for short-term energy storage occasions such as wave energy. Permanent magnet motors are the best choice for the conversion of electrical energy and flywheel kinetic energy in the energy storage flywheel system due to their advantages of small size and high efficiency. With the development of bearing technology, the

ISSN: 2414-1895 DOI: 10.6919/ICJE.202505_11(5).0005

rotational speed of the energy storage flywheel also increases, resulting in an increase in the frequency of current and magnetic field changes inside the motor, thereby increasing the iron loss and stator copper loss of the motor. The loss is dissipated in the form of heat, and due to the operation of the energy storage flywheel system in a vacuum condition, it is difficult for the heat generated by the motor loss to be conducted to the outside. The high temperature inside the energy storage system will lead to irreversible phenomena such as the failure of Hall sensors, coil burnout and demagnetization of the permanent magnet in the permanent magnet motor. Therefore, it is necessary to reduce the heat generation of the high-speed motor used in the energy storage flywheel. To reduce the iron loss of the flywheel system motor, Baowu Group, Shougang[4] and Japanese Metal[5] have developed extremely thin non-oriented silicon steel by increasing the silicon content, with a 53% reduction in iron loss compared to 35W300 at 10000r/min. Due to the inherent characteristics of silicon steel materials, the iron loss is inevitable. Li Zheng[6] conducted magnetic-thermal coupling analysis on the non-core permanent magnet linear motor and concluded that the high temperature of the motor would weaken the magnetic field strength of the permanent magnet. Shen Shunan[7] proposed an external transmission sub-ironless motor structure, where the stator uses non-magnetic materials, resulting in situations such as low magnetic density in the motor air gap. Wang Xiaoyuan[8] designed a PCB stator sub-ironless disc motor for application, adopting a double-rotor single-stator structure, which solved the problem of low magnetic density in the air gap of the sub-ironless motor, but the structure was complex and the processing cost was high.

In the process of motor optimization design, when multiple parameters are designed collaboratively, some scholars have adopted improved particle swarm algorithm, simulated annealing method and genetic algorithm to optimize permanent magnet motors[9-12]. Without the need for excessive finite element models, they can find the optimal parameters of the motor. However, the disadvantage is that the objective function is complex. Therefore, some studies have adopted Taguchi algorithm to establish orthogonal experimental matrix and conduct multivariable and multi-objective optimization for axial flux permanent magnet synchronous motors[13-15]. However, when there are many optimization parameters, it is easy to have contradictory parameters and it is not easy to achieve the optimal combination.

This paper designs an external-rotor high-speed permanent magnet motor with a rated power of 500W and a rotational speed of 10000r/min for energy storage flywheels. Firstly, a stator without core structure is proposed to address the heat problem caused by iron loss. Then, a model is established to analyze the loss situation. Secondly, a multi-objective optimization algorithm is adopted to enhance the torque and efficiency of the motor. This provides a reference for the design of statorless external rotor motors for energy storage flywheels.

2. Permanent Magnet Motor Design

2.1 Selection of Motor Type

Design a permanent magnet synchronous motor for energy storage flywheel with rated power of 500W and rated rotational speed of 10000rpm. Firstly, in order to reduce the wind friction loss of the flywheel, the interior of the flywheel housing is designed as a vacuum environment. Therefore, the designed permanent magnet motor needs to minimize heat generation as much as possible. Secondly, in order to improve the transmission efficiency, the rotor of the permanent magnet motor should be directly connected to the hub of the flywheel. The motor drives the rotating shaft, hub and rotational mass to rotate at high speed by its own torque.

Permanent Magnet Synchronous Motor (PMSM) has become an ideal drive motor for flywheel energy storage systems due to its small size and high power density. With the continuous advancement of motor topology, the design of PMSM has become more flexible, allowing for customized designs according to different working environments and requirements to meet increasingly complex and variable application scenarios. The requirements for this flywheel motor design include the following aspects:

ISSN: 2414-1895 DOI: 10.6919/ICJE.202505_11(5).0005

1) Direct drive of the flywheel. The rotor of the motor needs to be fixed on the flywheel to maintain the same rotational speed as the flywheel.

2) Low-loss motor type. Since the flywheel energy storage system is in a vacuum environment, air-cooling is not applicable for heat dissipation. Therefore, the design of the motor must have low losses to reduce heat generation.

The motors are mainly of the two structures as shown in Figure 1.

(a) Coreless disc-type permanent magnet (b) Coreless disc-type permanent magnet

Figure 1. Schematic diagram of coreless motor

The unique structure of the ironless disc-type permanent magnet motor consists of two rotating discs (rotors) and one stationary disc (stator). The rotating discs are equipped with permanent magnets, which can directly drive the flywheel to rotate and achieve energy storage and release. The stator winding is located between the two rotating discs. Although this thin-disc design enhances the power density of the motor and reduces its axial length, it also brings about the problem of heat dissipation. During the operation of the motor, the stator winding generates heat due to the current passing through it. However, because the winding is surrounded by two high-speed rotating rotating discs, the heat dissipation is restricted. Its stator is located between the two rotating discs, and the traditional support method is difficult to apply.

2.2 The Motor Only Requires a Certain Size.

In the design of an electric motor, the outer diameter of the stator and the effective radial dimension are regarded as the main dimensions of the motor.

$$\frac{D^2 l_{ef} n}{P} = \frac{6.1\times10^3}{\alpha'_p K_{Nm} K_{dp} A B_\delta} \tag{1}$$

Considering that this motor is constrained by the internal space of the flywheel housing, and the longer the axial length of the motor, the less favorable it is for the motor's heat dissipation.

The mainstream permanent magnet pole pairs of the motor are two-pole, four-pole and six-pole. The design target of the motor's rotational speed is 10000 r/min, and the upper limit of the output frequency of the existing driver board is 1000 Hz.

ISSN: 2414-1895 DOI: 10.6919/ICJE.202505_11(5).0005

$$N = \frac{60 \times f}{p} \tag{2}$$

In the formula, is the rotational speed of the motor (unit: RPM/min); is the power supply frequency (unit: Hz); is the pole pairs of the motor.

The more pole pairs the motor has, the smoother the output torque will be. After calculation, when the motor has four pole pairs, the required frequency is 666.7 Hz, which meets the design frequency of the driver board.

2.3 Motor Structure Design

The stator windings of the outer rotor permanent magnet motor can be classified into centralized windings and distributed windings. Their characteristics are shown in the following table. The winding method of the centralized windings is that each winding coil is wound between adjacent slots of the stator, that is, the span of the winding is 1. During the operation of the motor, the magnetic field of each phase winding mainly concentrates in the corresponding single slot area, and the position of the winding heating is relatively concentrated. The distributed windings are that each winding coil is distributed among multiple slots, and the span of the winding is determined according to the slot coordination of the motor pole. During the operation of the motor, the magnetic field generated by the distributed windings is relatively uniform, which can effectively reduce the fluctuation and harmonics of the magnetic field, and the position of the winding heating is relatively dispersed.

The stator of the ironless motor adopts non-magnetic material instead of the traditional silicon steel sheet material. The structure lacks the iron core to guide the magnetic field to pass through the air gap and the stator to form a closed circuit, resulting in disadvantages such as increased magnetic reluctance and magnetic flux dispersion in the magnetic circuit. Therefore, a magnetic conductor ring needs to be set inside the motor stator to ensure the integrity of the magnetic circuit. To avoid the iron loss caused by the magnetic conductor ring cutting the magnetic lines of force, the magnetic conductor ring inside the stator is combined with the outer rotor through the rotor support frame, thereby achieving the same-speed rotation of the two.

Since this design is for an ironless motor, the distance between the windings and the permanent magnets should be minimized as much as possible. Therefore, a single-layer winding design is adopted in this project. Resin materials have the advantages of high temperature resistance and corrosion resistance, and can be used for a long time within the temperature range of 280~450℃. Therefore, resin is selected as the stator material for this motor.

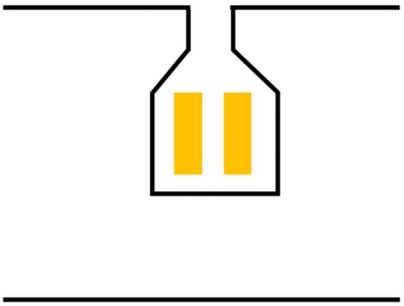

Figure 2. Stator slotting design

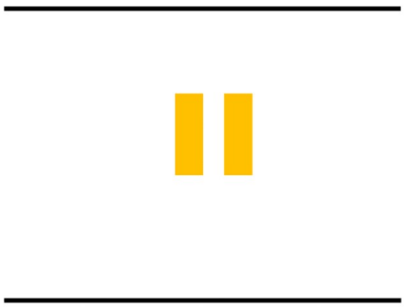

Figure 3. Slotless design of the stator

In this design, the number of stator slots is 24. The slot type of the motor is divided into two types. They are respectively Figure 2 and Figure 3.One is the traditional stator slot design, as shown in the

ISSN: 2414-1895 DOI: 10.6919/ICJE.202505_11(5).0005

figure below. In this design method, the windings in the stator slots cannot completely fill the space within the slots, and there will usually be a certain gap. The gap between the windings and the slot walls leads to an uneven magnetic field distribution, thereby affecting the efficiency and performance of the motor. Although the slot design makes the winding winding and installation relatively easy, the slots will damage the mechanical strength of the stator and affect the stability and service life of the motor.

3. Motor Optimization

The average output torque and torque fluctuation are two important indicators for evaluating the performance of a motor. According to the Maxwell electromagnetic simulation results of the motor in the previous chapter, the output torque of the motor is 428 mN/m, the torque fluctuation is 64 mN/m. This indicates that the torque fluctuation of the motor is relatively large and the fluctuation proportion is relatively high during its operation. Excessive torque fluctuation will have a series of adverse effects on the system, especially when it operates for a long time, it will have a significant impact on the service life and stability of the flywheel support shaft.

According to the modern theory of permanent magnet motor design, all parameters of the motor itself have an impact on the magnetic circuit of the motor, and this influence has both restrictive and promoting relationships. If a set of optimal parameters is obtained when optimizing the motor torque, but this set of data is not the optimal parameter in terms of torque fluctuation, then it is necessary to simultaneously optimize and analyze two or more targets.

3.1 Establishment of Response Surface for BP Neural Network

The air gap length directly affects the uniformity and intensity of the air gap magnetic flux density. A smaller air gap can increase the magnetic flux density, but it is also prone to causing problems of uneven magnetic flux density. The design of the magnetic isolation bridge affects the interaction between the permanent magnets in the rotor, thereby influencing the distribution and stability of the magnetic field. The shape of the magnetic conductor ring plays an important role in guiding the magnetic flux. Reasonable design of the magnetic conductor ring helps to optimize the magnetic flux path and reduce the uneven distribution of magnetic flux density. The shape and layout of the permanent magnets also determine the distribution of the magnetic field. Reasonable design can effectively improve the uniformity of the air gap magnetic flux density and reduce torque fluctuations. Optimizing these design parameters in flywheel permanent magnet motors helps to increase the output torque of the motor, shorten the acceleration time of the flywheel during the charging stage, reduce torque fluctuations, and improve the overall stability of the system.

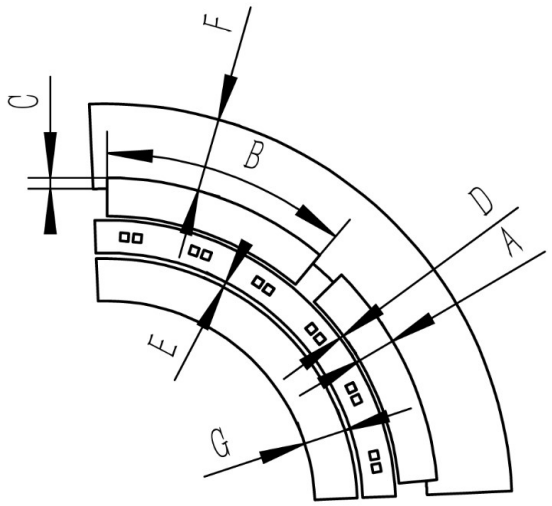

Figure 4. Parameter selection of flywheel permanent magnet motor

ISSN: 2414-1895 DOI: 10.6919/ICJE.202505_11(5).0005

Based on the above content, select the following parameters: thickness of the permanent magnet A, angle of the permanent magnet B, length of the magnetic insulation bridge C, gap length between the outer rotor and the stator (gap one) D, gap length between the magnetic conductor ring and the stator (gap two) E, thickness of the outer rotor iron core F, and thickness of the magnetic conductor ring iron core G. As shown in Figure 4 below.

BP neural network is more adept at analyzing nonlinear relationships and high-dimensional problems in the model. With the improvement of computer hardware performance, the application of BP neural network in model prediction has become more widespread. The structure of BP neural network includes the input layer, output layer and hidden layer. The number of hidden layers is proportional to the prediction effect and inversely proportional to the computational complexity. The fitting object of this optimization is a medium and small-sized motor, so a single-layer hidden layer is selected.

(1) Input layer. This chapter mainly analyzes the influence of the thickness of the permanent magnet, the angle of the permanent magnet, the length of the magnetic isolation bridge, the length of air gap 1, the length of air gap 2, the thickness of the outer rotor core and the thickness of the magnetic conductor ring on the torque of the motor. Therefore, the number of input layer nodes of this BP neural network is 7, corresponding to these parameters respectively.

(2) Output layer. The output layer is the target output result after BP neural network training. The objective of this motor optimization is the output torque and the torque fluctuation, so the number of output layer nodes of BP neural network is 2, and the linear activation function (purelin) is used for output.

(3) Hidden layer. The hidden layer is located between the input layer and the output layer. This is the core part of BP neural network. The role of the hidden layer is to convert the input data into more abstract feature representations through weighted summation and activation functions. By adjusting the weights of the parameters and using the hyperbolic tangent Sigmoid activation function (tansig) for nonlinear transformation, the fitting accuracy and accuracy of the model are improved.

Since the optimization parameters for this time are set to 7 groups, Ansys Maxwell is adopted for rapid modeling as the basis of the BP neural network model. 1000 sets of finite element analysis data are calculated. After obtaining the finite element simulation data set, it is input into the BP neural network model and compared with the actual values to obtain the predicted output values. The comparison results are shown in the following table.

Table 1. BP neural network response surface experiment

	1	2	3	4	5
Thickness of permanent magnet (mm)	6.8	7.1	7.3	6.6	7.2
Angle of permanent magnet (°)	39.5	40.2	39.5	40.5	40.7
Length of air gap 1 (mm)	0.7	0.65	0.89	0.75	0.83
Length of magnetic insulation bridge (mm)	4	4	4	4	4
Length of air gap 2 (mm)	1	1	1	1	1
Thickness of rotor core (mm)	14	14	14	14	14
Thickness of magnetic conductor bridge (mm)	8	8	8	8	8
Predicted torque value (mN/m)	421.4	438	429	418.6	435.9
Actual torque value (mN/m)	421.5	438.4	429.2	418.8	436.6
Predicted torque fluctuation value (mN/m)	102.7	127.3	79.8	129.6	123.5
Actual torque fluctuation value (mN/m)	101.6	126.2	78.6	128.5	122.3

ISSN: 2414-1895 DOI: 10.6919/ICJE.202505_11(5).0005

The fitting accuracy of the BP neural network experiment was verified by using five sets of test points. The group with the smallest error in the measurement of the output torque of the motor was the first group, with the torque error being less than 0.02%, while the group with the largest prediction error was the second group, with the error being 0.09%. The group with the smallest prediction error for the torque fluctuation was the first group, with the torque error being 1.08%, and the group with the largest prediction error was the third group, with the error being 1.53%.

3.2 Improved NSGA-II Algorith

In the traditional NSGA-II algorithm, due to the over-concentration of the population, situations where individual differences are small often occur, which leads to the solution set being prone to tend towards a specific direction during crossover, mutation and selection. This results in the algorithm getting stuck in local optima at the initial stage. When there are multiple local optima in reality, due to the limitation of the algorithm's search range, some areas are not searched, thereby reducing the diversity of the solution set. The chaotic phenomenon describes the phenomenon that seems random but actually contains patterns in reality, such as the famous "Butterfly Effect". Introducing the random and ergodic characteristics of chaos theory into the NSGA-II algorithm can effectively solve the problem of uneven distribution of the solution set during population initialization. Introducing chaotic search into the target search process helps to enhance the algorithm's search ability in different regions and improve the global search efficiency.

In NSGA-II, the initialization of the population is usually random. However, chaos search can be used to generate a more uniform and widely distributed initial population. By introducing chaotic sequences, the distribution of individuals within the population is no longer completely random but based on the rules of the chaotic system, which can cover a larger search space and thereby enhance the global search ability of the algorithm.

$$\begin{cases} 6.5 \le A \le 7.5 \\ 39^\circ \le B \le 41^\circ \\ 2 \le C \le 6 \\ 0.6 \le D \le 1 \\ 0.8 \le E \le 1.2 \\ 13 \le F \le 15 \\ 7 \le G \le 9 \end{cases} \tag{3}$$

In order to ensure that the results of multi-objective optimization are in line with the actual situation of the motor, a penalty function is introduced. When the algorithm provides an unreasonable solution, the penalty score of the current solution is directly increased in a way to effectively prevent the algorithm from getting stuck in an invalid solution.

$$\begin{cases} 300 < T_{out} < 460 \\ 0 < T_w < 200 \end{cases} \tag{4}$$

3.3 Optimization Results of the Improved NSGA-II Algorithm

As shown in Figure 5 above,by optimizing the parameters of the motor through comparison, the average output torque of the motor increased from 428.9 mN/m to 451.2 mN/m, an increase of approximately 5.2%. The torque fluctuation decreased from the original 64.0 mN/m to 61.8 mN/m, a reduction of 3.4%.

ISSN: 2414-1895 DOI: 10.6919/ICJE.202505_11(5).0005

Table 2. Comparison of Data Before and After Optimization

	Before optimization	After optimization
Thickness of permanent magnet (mm)	7	7.48
Angle of permanent magnet (°)	40	39.49
Length of air gap 1 (mm)	0.75	0.78
Length of magnetic insulation bridge (mm)	2	2.37
Length of air gap 2 (mm)	1	0.86
Thickness of rotor core (mm)	14	14.91
Thickness of magnetic conductor bridge (mm)	7.7	7.93
Predicted torque value (mN/m)	428.9	451.2
Predicted torque fluctuation value (mN/m)	64.0	61.8

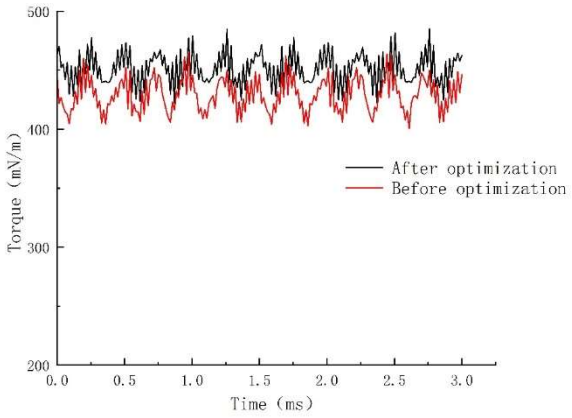

Figure 5. Torque comparison before and after the optimization

4. Conclusion

This paper mainly focuses on the high-speed permanent magnet synchronous motor used for flywheel energy storage as the research object, and conducts an optimization analysis on its internal structure, magnetic circuit, and torque. The main work is as follows:

(1) Preliminary design of the high-speed permanent magnet motor for flywheel energy storage. In response to the requirements of low heat generation and high efficiency for the motor used in flywheel energy storage, an open stator motor without core is selected. Then, the requirements of the flywheel energy storage system for the motor's torque, speed, and power are calculated. Based on these requirements, the main dimensions, the number of pole pairs of the permanent magnets, the number of stator slots, and the supporting structure of the motor are designed. Finally, the air-gap magnetic density and torque fluctuation of the designed motor are analyzed.

(2) Investigate the parameters influencing the torque characteristics of the motor. Through analysis, it is found that the parameters affecting the torque of the motor include the thickness of the permanent magnet, the angle of the permanent magnet, the length of the magnetic isolation bridge, the air gap length between the outer rotor and the stator, the air gap length between the magnetic conductor ring and the stator, the thickness of the outer rotor core, and the thickness of the magnetic conductor ring core. By establishing a BP neural network response surface, after testing, the results show that the BP neural network has a good fitting of the response surface for complex parameters.

ISSN: 2414-1895 DOI: 10.6919/ICJE.202505_11(5).0005

(3) Improve the NSGA-II algorithm. In view of the problem that the NSGA-II algorithm is prone to fall into local optimum, chaotic initialization is introduced in the initialization of the algorithm population, and chaotic search is introduced in the algorithm space search. After testing, the improved algorithm has a better convergence effect than the previous one. Finally, the torque characteristics of the optimized motor are analyzed through finite element comparative analysis. The torque is increased by 5.2%, and the torque fluctuation is reduced by 3.4%.

References

[1] Fu Qiang. Application of Energy Storage Technology in Wind Power and Photovoltaic Systems [J]. China High-Tech, 2024, (16): 111-113.

[2] Huang Yuhuanch, Ding Tao, Li Yuting, et al. Review of Energy Low-carbonization Technologies under the Context of Carbon Neutrality and Implications for the Development of New Power System [J]. Proceedings of the CSEE, 2021, 41(S1): 28-51.

[3] Xie Xiaorong, Ma Ningjia, Liu Wei, et al. Review and Prospect on the Application Functions of Energy Storage in New Power System [J]. Proceedings of the CSEE, 2023, 43(01): 158-169.J. Liu, E.L. Chen and Z.T. He: Journal of Shi Jia Zhuang Railway Institute (Natural Science), Vol. 22 (2009) No. 4, p.40-42.

[4] Fan Lifeng, Qin Meimei, Yue Erbin, et al. Technical Challenges of New Energy Vehicles to Non-oriented Silicon Steel [J]. Materials in China, 2021, 35(15): 15183-15188.

[5] Ueno S, Enokizono M, Mori Y, et al. Vector magnetic characteristics of ultra-thin electrical steel sheet for development of high-efficiency high-speed motor[J]. IEEE Transactions on Magnetics, 2017, 53(11): 1-4.

[6] Li Zheng, Yue Feihong, Wang Lei Yong, et al. Electromagnetic-Thermal-Stress Coupling Analysis of Permanent Magnet Synchronous Linear Motor Without Core [J]. Micro-Motors, 2019, 52(04): 1-6.

[7] Shen Shunan, Zhu Hanqiu. Parameter Optimization Design of Outer-Rotor Permanent Magnet Synchronous Motor without Core and Bearing [J]. Micro-Motors, 2021, 54(05): 20-26. DOI: 10.15934/j.cnki.micromotors.2021.05.005.

[8] Wang Xiaoyuan, Li Xiang, Pang Wei, et al. Comparative Analysis of Distributed Windings in PCB Stator Coreless Disc Motors [J]. Journal of Electrical Machines and Control, 2018, 22(11): 11-18.

[9] He Chao. Design and Optimization of Disc-Type Ironless Permanent Magnet Synchronous Motor Based on PCB Winding [D]. Shanghai Institute of Electric Power, 2018.

[10] Zhang Fengge, Du Guanghui, Wang Tianyu, et al. Review on the Development and Design of High-speed Motors [J]. Transactions of China Electrotechnical Society, 2016, 31(07): 1-18.

[11] Xing Liying, Bao Jianwen, Li Songming, et al. Current Development Status and Challenges of Advanced Resin-Based Composites [J]. Journal of Composite Materials, 2016, 33(07): 1327-1338.

[12] Ye Jinhu. Principles and Design of Modern Brushless DC Permanent Magnet Motors [M]. Beijing: Science Press, 2007.

[13] Xie Yu. Temperature Field Analysis of High-speed Permanent Magnet Synchronous Motor for Flywheel Energy Storage [D]. Tianjin University, 2017.

[14] Lu Qinfen, Shen Yiming, Ye Yunyue. Review on the Structure and Research Development of Permanent Magnet Linear Motors [J]. Proceedings of the CSEE, 2019, 39(09): 2575-2588.

[15] Zong Kefang, Zhao Jiwen, Song Juncai, et al. Thrust Fluctuation Suppression Based on V-Type Coil Permanent Magnet Synchronous Linear Motor [J]. Proceedings of the CSEE, 2019, 39(22): 6736-6746.